Heterocyclic Letters
Vol. 13| No.4|715-728|Aug-Oct|2023
ISSN : (print) 2231–3087 / (online) 2230-9632
CODEN: HLEEAI
http://heteroletters.org

SYNTHESIS AND ANTIOXIDANT EVALUATION WITH *IN SILICO* STUDIES OF QUINONE HYDRAZONES

Dhangapure Rohit[a], Harnekar Fahad[a], Kulkarni Prafull[a], Shilimkar Suyash[a], Tambe Pranav[b], Khursheed Ahmed[a] and Pangal Anees[a]*

[a]*Advanced Scientific Research Laboratory, Department of Chemistry and Post Graduate Centre, Abeda Inamdar Sr. College of Arts, Science & Commerce (Autonomous), Camp, Pune – 411001, India*
[b]*Department of Biotechnology, Abeda Inamdar Sr. College of Arts, Science & Commerce (Autonomous), Camp, Pune – 411001, India*
**Corresponding Author: E-mail: pangalanees@azamcampus.org*

ABSTRACT:
We report the synthesis, structural characterization and antioxidant activity of biologically active hydrazones**Q-1** to **Q-5** from2,6-di-*tert*-butyl-1,4-benzoquinone and hetero aromatic hydrazides. The hydrazone, **Q-2** shows a notable antioxidant potential of 9.09 ± 0.48 µg/ml as compared to ascorbic acid. All the derivatives were screened virtually for ADMET, physicochemical properties, drug likeness and molecular docking studies. These hydrazones showed good pharmacodynamics and physicochemical properties, as well as no violations in drug-likeness predictions. These compounds were further subjected for possible target prediction and the compounds were found to target enzymes in the biological systems. Further, these compounds were docked in COX-2 (PDB Id: 6COX) protein and found to exhibit reasonably good interactions with amino acid residues, showed a good binding energy and fit favorably into the 6COX active site displaying hydrogen bonding with different amino acid residues of the target protein. The experimental results of the antioxidant activity fit well with the predicted *in silico* results. Therefore, these new derivatives (**Q-1** to **Q-5**), containing a quinone and an azomethine group, can become good drug candidate for designing new drug and can be considered for further optimization and lead development.

KEYWORDS: Quinone, Hydrazone, *In silico*, ADMET, Drug-likeness, Molecular docking.

INTRODUCTION:

Schiff base products or hydrazones are generally known as azomethine or imine compounds due to the presence of azomethine bond (C=N), are derived from the condensation of an acid hydrazides and aromatic aldehydes or ketones and generally catalyzed by acid or base or on thermal treatment. Schiff bases are widely used and the most treasured organic building block

with diversified pharmacological properties and promising potential in biological, clinical, analytical and industrial applications[i]. Generally, these compounds contain the azomethine group and the growing interest in the chemistry of hydrazones is related to their wide spectrum of bioactivities.Many organic compounds containing the azomethine group have been synthesized and tested for their biological activities, proving very effective as antimicrobial, antibacterial, antifungal, antiviral, antiinflammatory and anticancer[ii].

Quinones are naturally occurring compounds and various synthetic compounds have been a part of various biological processes as well as performing a variety of functions e.g. coenzyme Q10 functions as an electron carrier in the respiratory chain, Vitamin K is essential for blood coagulation and juglone and plumbagin exhibits growth inhibitory effects on microorganisms and are used by plants as defensive compounds[iii]. Many reports are available exploring diverse pharmacological properties of quinones such as anti-inflammatory[iv], antimicrobial[v], anticancer[vi-viii], antiallergic and antiplatelet[ix-x], antibacterial[xi], antifungal[xii], antithrombotic[xiii], antiringworm[xiv], and antiviral agents[xv]. On the other hand, the heterocyclic moieties have wide scale practical applications starting from extensive clinical use to diverse fields like medicine, agriculture, photochemistry and polymer science[xvi]. Heterocyclic compounds are the exceptional targets for anticancer research and drug discovery. Among them, nitrogen containing compounds have shown excellent effects than non-nitrogen containing compounds[xvii]. Different heterocyclic compounds like furan, thiophene, pyrrole and pyridine scaffolds have been found in numerous cytotoxic agents[xviii]. The Pyridine ring is a component of several important natural products such as nicotine and nucleic acid. Nicotinic acid and its derivatives have gained an immense importance in the development of drugs on account of the wide variety of biological properties displayed by them. The compounds containing furan and thiophene nucleus exhibit diverse biological properties. Several furan-based derivatives exhibit potent biological activitiesand thiophenes are found in many natural products which exhibit cytotoxic activity against several cancer cell types[xix-xxiii]. However, Computer aided drug design (CADD) methods are useful to identify and develop a potential lead in the new drug design and discovery. Absorption-Distribution-Metabolism-Excretion (ADME) studies are utilized in the drug development process to examine numerous factors which influence on drug activity and availability. These evaluations are important to raise a researcher's knowledge to understand the behavior of a candidate drug[xiv-xv]. Quinone have several attractive features, such as low molecular weight, simple structure, high bioavailability, high solubility in most of the organic solvents and low toxicity, which, together with their multifaceted biological activities, ensure them a prominent role as lead compounds in drug research and development[xvi].

Keeping in view the hybrid concept and the great biological potential of quinone scaffolds, we planned to synthesize new hydrazones with different heteroaryl hydrazides, to evaluate their biological properties and to study their pharmacokinetic, physicochemical properties and drug likeness by *in silico* computational methods. In the present work, we synthesized the new hydrazones from 2,6-di-*tert*-butyl-1,4-benzoquinone and screened for their antioxidant potential by using DPPH free radical scavenging method. Additionally, all the synthesized compounds were subjected to the *in silico* methods to determine ADMET, physicochemical properties and drug likeness, target prediction and binding affinities using online sources.

EXPERIMENTAL:

Syntheses of 2,6-di-*tert*-butyl-1,4-benzoquinone hydrazones:

Solvents for synthesis were reagent grade and dried by standard procedures. The starting materials such as 2,6-di-*tert*-butyl-1,4-benzoquinone and different heteroaryl hydrazides were obtained from Sigma-Aldrich chemicals and acetone, methanol, ethanol and Trifluoroacetic

acid (TFA) were obtained from Loba Chemical Limited, India. Melting points of as synthesized compounds were determined with open capillary tube on a VEEGO melting point apparatus. The IR, ^{1}H-NMR and Liquid chromatography mass spectra (LCMS) were obtained from Central Instrumentation Facility, Savitribai Phule Pune University (SPPU), Pune.

The synthetic methodology employed for the synthesis of target compounds is illustrated in **Figure 1**. To the solution of 2,6-di-*tert*-butyl-1,4-benzoquinone **(1**, 1 eq.**)** and different heteroaryl hydrazides (**2**, 1eq) in ethanol, 5-6 drops of trifluoroacetic acid were added and the mixture was stirred at room temperature. After completion of the reaction as monitored by TLC, the reaction mixture was poured into the cold water and the solid obtained was filtered and washed with cold ethanol and recrystallized from ethanol.

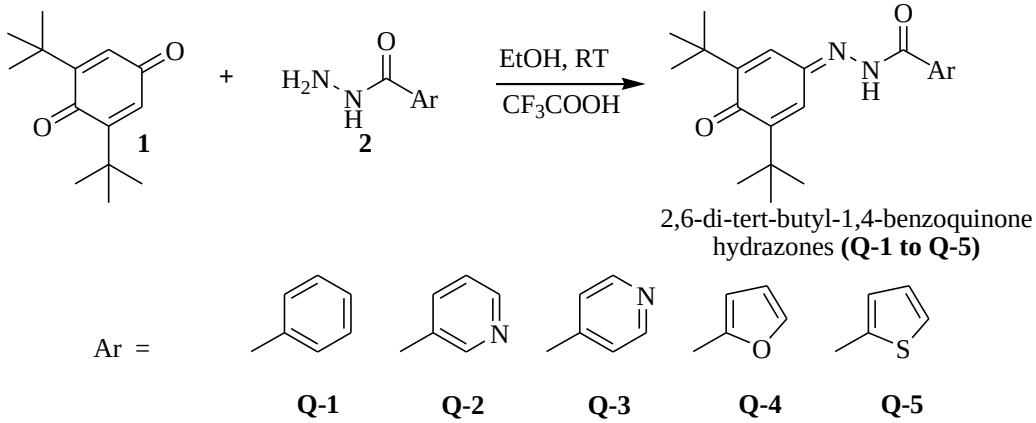

Figure 1: Synthesis of 2,6-di-*tert*-butyl-1,4-benzoquinone hydrazones

1) *N'-(3,5-di-tert-butyl-4-oxocyclohexa-2,5-dienylidene)benzohydrazide* (**Q-1**)**:** Pale yellow, yield (90%), MP 278-280 ^{O}C; LCMS (EI+): $C_{21}H_{26}N_2O_2$: 339.1;IR (KBr, cm^{-1}):3186.90 (-NH), 3021.08 (-CH), 1658.31 (>C=O), 1548.07 (-C=N-);^{1}H-NMR (500 MHz, DMSO) δ: 1.29 (s, 18H), 12.23 (s, -NH, 1H), 7.17 (s, olefinic, 2H), 7.87 (d, J = 7.5Hz, 2H),), 7.64 (t, J = 7.5 Hz and 7.5 Hz, 1H), 7.56 (t, J = 7.5 Hz and 7.5 Hz, 2H).

2) *N'-(3,5-di-tert-butyl-4-oxocyclohexa-2,5-dienylidene)nicotinohydrazide*(**Q-2**)**:**Yellow, yield (75%), MP 124-126 ^{O}C;LCMS (EI+): $C_{20}H_{25}N_3O_2$: 339.9;IR (KBr, cm^{-1}):3265.16 (-NH), 2958.17 (-CH), 1660.41 (>C=O), 1547.56 (-C=N);^{1}H-NMR (500 MHz, DMSO)δ: 1.29 (s, 3H), 12.54 (s, 1H, -NH), 6.74-9.02 (m, 6H).

3) **3)***N'-(3,5-di-tert-butyl-4-oxocyclohexa-2,5-dienylidene)isonicotinohydrazide* (**Q-3**): Yellow, yield (78%), MP 128-130^{O}C; LCMS (EI+): $C_{20}H_{25}N_3O_2$: 340.1;IR (KBr, cm^{-1}):3385.12 (-NH), 2963.49 (-CH), 1662.02 (>C=O), 1525.42 (-C=N);^{1}H-NMR (500 MHz, DMSO) δ: 1.29 (s, 18H), 12.54 (s, -NH, 1H), 7.25 (d, olefinic, 2H), 8.12 (dd, J = 7.5Hz and J=2.5Hz, 2H), 7.75 (dd, J = 7.5Hz and J=2.5Hz, 2H).

4) *N'-(3,5-di-tert-butyl-4-oxocyclohexa-2,5-dienylidene)furan-2-carbohydrazide*(**Q-4**)**:** Yellow, yield (90%), MP 208-210 ^{O}C; LCMS (EI+): $C_{19}H_{24}N_2O_3$: 328.8;IR (KBr, cm^{-1}):3370 (-NH), 2958.27(-CH-), 1658.95 (>C=O), 1551.45 (-C=N);^{1}H-NMR (500 MHz, DMSO) δ: 1.29 (s, 18H), 12.33 (s, 1H, -NH), 7.720 (s, 2H, olefinic), 8.237 (s, 1H, furyl), 9.02 (s, 1H, furyl), 7.59 (s, 1H, furyl).

5) *N'-(3,5-di-tert-butyl-4-oxocyclohexa-2,5-dienylidene)thiophene-2-carbohydrazide*(**Q-5**): Yellow, Yield (92%), MP 210-212^{O}C; LCMS (EI+): $C_{19}H_{24}N_2O_2S$: 344.8;IR (KBr, cm^{-1}):3291.89 (-NH), 2968.87 (-CH), 1669.70 (>C=O), 1504.20 (-C=N);^{1}H-NMR (500 MHz, DMSO)δ: 1.29 (s, 18H), 12.23 (s, 1H, -NH), 7.65 (d, 2H, olefinic), 8.04 (s, 1H, thiophenyl), 7.05 (s, 1H, thiophenyl), 6.75 (s, 1H, thiophenyl).

General procedure for antioxidant activity:

The antioxidant activity of the synthesized hydrazones was determined by using 1,1- diphenyl picryl hydrazyl (DPPH) assay method as explained by Pangal*etal.*[xxv] with slight modifications. Drug stock solution (1000 µg/ml) was diluted to final concentrations of 1, 5, 10, 20, 30, 40, 50, 60, 70, 80, 90 and 100 µg/ml in methanol. About 0.004 g DPPH reagent was dissolved in 100 ml methanol. In 96-well plates, 50µl sample and 150 µl DPPH solution were added. The plate was incubated for 30 min at room temperature in the dark, and finally, absorbance was recorded at 520 nm wavelength and converted into the percentage antioxidant activity. Methanol was used as the solvent and ascorbic acid as the standard. The percent radical scavenging was calculated from the absorbance using the following formula –

$$\%\ \text{Radical scavenging activity} = \frac{(\text{Abs of control} - \text{Abs of sample})}{\text{Abs of control}} \times 100$$

General procedure for *in silico* methods:

The designed synthesized 2,6-di-*tert*-butyl-1,4-benzoquinone derivatives (**Q-1 to Q-5**)were subjected to an *in silico* screening for ADMET, pharmacokinetic, physicochemical and drug-likeness properties, target prediction, toxicity prediction and molecular docking using the computational tools the pkCSM, SwissADME, ProTox-II and CB-Dock2 as online tools[xvii]. These web servers were selected because they are freely accessible and provide strongly built computational methods to estimate a universal judgment of the pharmacokinetics and toxicity of small molecules.

ADMET Prediction: The ADMET studies are significant to estimate the pharmacodynamics of the designed compounds, which could be a candidate agent in drug design and discovery studies. SMILES format of the designed molecules are uploaded on the pKCSM web server (https://biosig.lab.uq.edu.au/pkcsm/prediction). The pkCSM web server provide the information with respect ADMET parameters like gastrointestinal (GI) absorption, blood-brain barrier (BBB) permeability, CYP2D6 and CYP3A4 substrates and inhibitors, human skin permeability coefficients (log Kp), Caco-2 permeability, volume of distribution at steady state (VDss), CNS permeability, total clearance, AMES toxicity, maximum recommended tolerated dose (MRTD) human, oral rat acute toxicity (LD50) and hepatotoxicity, skin sensitization etc.

Pharmacokinetic, physicochemical properties and drug-likeness prediction: The designed molecules were estimated for pharmacokinetic, physicochemical properties and drug-likeness properties using SwissADME (http://www.swissadme.ch/). SwissADME is a web-based platform that lets users upload or draw their target compounds with structure or SMILES code. This tool supplies many parameters like lipophilicity (iLOGP, XLOGP3, WLOGP, MLOGP, SILICOS-IT, Log Po/w), water solubility – Log S (ESOL, Ali, SILICOS-IT), drug-likeness rules (Lipinski, Ghose, Veber, Egan, and Muegge) and Medicinal Chemistry (PAINS, Brenk, Leadlikeness, Synthetic accessibility) methods.

Target Prediction: SMILES codes of the designed compounds were uploaded to the SwissTargetPrediction website (https://www.swisstargetprediction.ch) to analyze their putative off-targets in the human organism.

Molecular Docking: In order to understand the probable binding affinities of the synthesized derivatives, molecular docking studies were carried out at active site of human cyclooxygenase (COX-2) enzyme (PDB ID: 6COX) using online molecular docking platform CB-Dock2 (https://cadd.labshare.cn/cb-dock2). The docking results were saved as PDB file and the PDB were processed to observe the interactions according to the literature.

RESULTS AND DISCUSSIONS

Chemistry:

Melting points of the synthesized compounds were determined with open capillary tube on a VEEGO melting point apparatus and are uncorrected. The ^{1}H-NMR spectra were obtained on a 500 MHz and the LCMS were obtained on a Agilent LCMS from CIF, SPPU, Pune.

The structures of the synthesized 2,6-di-tert-butyl-1,4-benzoquinone hydrazones, **Q-1** to **Q-5** were confirmed by their mass and spectral analyses. The LCMS (ESI) spectra of the synthesized analogs showed major peaks corresponding to expected M+1 fragment at 339.1, 339.9, 340.1, 328.8 and 344.8 respectively. The ^{1}H-NMR spectrum of the synthesized analogs showed proton of the –tertiary butyl group at 1.29 ppm. The olefin proton on quinones appeared as at about 8.2 ppm. On the other hand, the protons of –NH groups appeared as singlet in the range of 12.22 to 12.54 ppm. In the IR spectrum, thesehydrazones showed a peak in between 3186 to 3385 cm^{-1} due –NH.The peak in between 1658 to 1669 cm^{-1} is due to>C=Oand –C=N-group appeared in between 1504 to 1551 cm^{-1}.

Antioxidant Activity:

All the synthesized hydrazones were evaluated for their antioxidant activity using 96 well plate method. In general, 50 µl samples (1 to 100 µg/ml) and 150 µl of 0.004% DPPH solution were mixed together in 96 well plate and the plates were incubated for 30 minutes and dark. After 30 minutes the absorption was measured at 520 nm. The graph of % scavenging activity versus concentration of bis – hydrazones was plotted and presented in **Figure 2**. The IC_{50} concentration values were determined from an online source (http://www.ic50.tk). The results obtained were compared with IC_{50} value of standard ascorbic acid. The results revealed that Q-3 and Q-4 among the compounds were highly active. Similarly, other analogs showed good antioxidant activity when compared with the standard. The scavenging effect increased with the increasing concentrations of test compounds. The IC_{50} value for standard drug ascorbic acid and all synthesized hydrazones were 8.68 ± 0.40, 15.29 ± 0.64, 9.09 ± 0.48, 11.9 ± 0.74, 12.2 ± 0.54 and 14.28 ± 0.53µg/mlrespectively which were comparable to the IC_{50} value of std. drug ascorbic acid. Among these analogs, Q-4 exhibited best antioxidant activity with lowest IC_{50} value than other analogs. The results of DPPH activity showed that these hydrazones are equally effective as antioxidant compared to ascorbic acid.

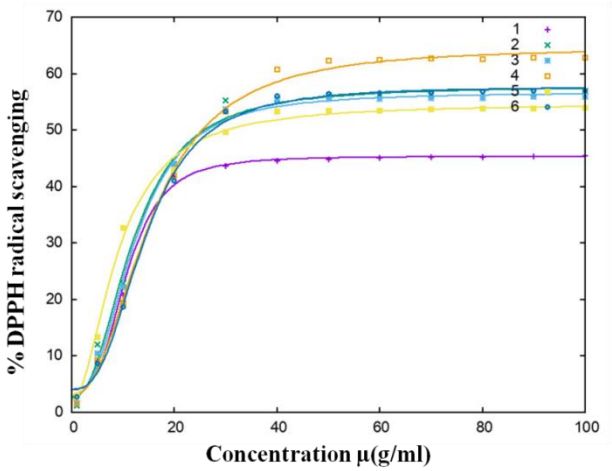

Figure 2: Antioxidant activity curves of hydrazones (Q-1 to Q-5)
(1= STD, 2 = Q-1, 3 = Q-2, 4 = Q-3, 5 = Q-4, 6 = Q-5)

***In silico* evaluation methods:**

ADMET Prediction: The predicted pharmacokinetic parameters and other physicochemical properties are important for both *in silico* and *in vitro* evaluation of drug-like properties. To make sure that the synthesized molecules show the potential of a drug, their ADMET properties were checked using pkCSM and the predicted values are shown in **Table 1.** All of the derivatives were found to show good solubility values in water. The values greater than 0.90 for the Papp coefficient and more than 30% intestinal absorption indicate the compound's high Caco-2 permeability and good gastrointestinal absorption. All the derivatives showed a good Caco-2 permeability and great gastrointestinal absorption. The values of skin permeability, VDss (human) and CNS permeability are in the permitted range. The inability of the molecule to inhibit CYP2D6 and CYP3A4 shows that all the derivatives will not allow the metabolism of xenobiotics in the body. The values of total clearance are quite favorable for all **Q-1** to **Q-4** indicating non-toxic behavior. The derivative except **Q-5** which will not be eliminated from the body and this may be associated with certain types of toxicities. The hydrazones showed hepatotoxicity except **Q-4** and the derivatives **Q-1** and **Q-5** are skin sensitive. Furthermore, all these hydrazones act as non-carcinogenic which is depicted from negative AMES toxicity test. These overall results of ADMET studies disclosed that the compounds have good pharmacokinetic properties.

Table 1:ADMET properties of hydrazones (Q-1 to Q-5) calculated from pkCSM

Property	**Model Name**	**Q-1**	**Q-2**	**Q-3**	**Q-4**	**Q-5**
Absorption	Water solubility[a]	-5.457	-5.018	-5.191	-4.772	-5.561
	Caco-2 permeability[b]	1.225	0.936	0.944	0.865	1.45
	Intestinal absorption (human)[c]	92.114	94.431	94.431	92.98	90.59
	Skin Permeability[d]	-2.829	-3.055	-3.057	-2.881	-2.856
Distribution	VDss (human)[e]	0.205	-0.077	-0.062	-0.005	0.064
	Fraction unbound (human)	0	0.061	0.058	0.1	0
	BBB permeability[f]	-0.027	-0.225	-0.225	-0.189	-0.053
	CNS permeability[g]	-1.626	-1.883	-1.895	-1.82	-1.673
Metabolism	CYP2D6 inhibitor[h]	No	No	No	No	No
	CYP3A4 inhibitor[h]	No	No	Yes	No	No
Excretion	Total Clearance[i]	0.492	0.481	0.536	0.575	-0.036
Toxicity	Max. tolerated dose (human)	-0.712	-0.382	-0.363	-0.464	-0.761

	Oral Rat Acute Toxicity (LD50)[j]	2.416	2.362	2.361	2.543	2.549
	Oral Rat Chronic Toxicity (LOAEL)	1.904	1.106	1.113	1.025	0.903
	Minnow toxicity[k]	-0.174	0.043	0.294	0.542	-0.07
	Hepatotoxicity[h]	Yes	Yes	Yes	No	Yes
	Skin Sensitization[h]	Yes	No	No	No	Yes
	AMES toxicity	No	No	No	No	No

Note:[a](log mol/L), [b](log Papp in 10^{-6} cm/s), [c](% Absorbed), [d](log Kp), [e](log L/kg), [f](Fu), [g](log PS), [h](Yes/No), [i](log ml/min/kg), [j](LD50 in mol/kg), [k](LOAEL in log mg/kg_bw/day)

Furthermore, the BOILED-Egg profile **(Figure 3)** enables the perceptive consideration of passive gastrointestinal absorption (HIA) and brain penetration (BBB) in the function of the position of the molecules in the WLOGP-vs-TPSA referential and was screened for these five compounds. In this model, the white area corresponds to a high probability of passive absorption in the GIT, while the yellow area is for a high probability of brain penetration. Also, the marks are colored in blue if predicted as actively effluxes by P-gp (PGP+) and in red if estimated as non-substrate of P-gp (PGP−). All designed compounds were estimated to be well-absorbed but not accessing the brain, and all compounds were not subject to active efflux (red dot).

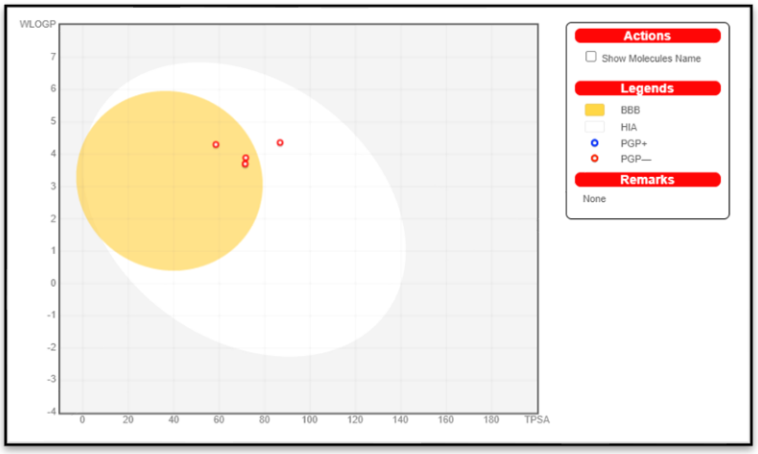

Figure 3: BOILED-Egg presentation of hydrazones (Q-1 to Q-5)

The physicochemical properties and drug-likeness prediction:

The physicochemical properties give a comprehensive depiction of the structures of derivatives such as molecular weight (MW), molar refractivity (MR), topological polar surface area (TPSA), number of rotatable bonds, heavy atoms and hydrogen bond acceptors and donors. The physicochemical properties of the synthesized quinone derivatives (Q-1 to Q-5) were predicted by using the SwissADME and the results are presented in **Table 2**. The bioavailability properties exhibited by the analogs are within the range which makes them orally bioavailable and excellent drug candidates. The bioavailability predictions of the compounds displayed a rapid evaluation of drug likeness. The drug likeness was evaluated based on the physicochemical properties to find oral drug candidates. There are five different rule-based filters which are used to predict whether the chemical compounds can act as drug. The result of drug likeness evaluation of analogs is shown in **Table 3** –

Table 2: Physicochemical properties of hydrazones (Q-1 to Q-5)

Properties		**Q1**	**Q2**	**Q3**	**Q4**	**Q5**
Molecular weight (g/mol)		338.44l	339.43	339.43	328.41	344.47
No. of Heavy atoms		25	25	25	24	24
No. of Arom. heavy atoms		6	6	6	5	5
No. of Rotatable bonds		5	5	5	5	5
No. of H-Bond acceptors		3	4	4	4	3
No. of H-Bond donors		1	1	1	1	1
Molar Refractivity		102.23	100.03	100.03	94.50	100.11
Total polar surface area Å²		58.53	71.42	71.42	71.67	86.77
Solubility	**Log S (ESOL)**	-4.84	4.17	-4.17	-4.37	-4.86
	Log S (Ali)	-5.80	4.96	-4.96	-5.46	-6.41
	Log S (SILICOS-IT)	-5.88	-5.50	-5.50	-5.10	-5.14
Lipophilicity	**MLOGP**	3.29	2.24	2.24	2.05	2.88
	WLOGP	4.30	3.70	3.70	3.89	4.36
	XLOGP3	4.84	3.77	3.77	4.24	4.85

All the test compounds showed good drug similarity and can be a good drug candidates. They have no violations for drug likeness as per the laws framed by Lipinski, Ghose, Veber, Egan and Muegge. The Brenk and Pan Assay INterferencecompoundS (PAINS) structural alerts used in medicinal chemistry for the identifying unstable, reactive, toxic fragments present in the structure. Among the compounds examined, all molecules resist Brenk's rule due to quinone moiety and an imine group. These derivatives also showed one alert in PAINS due to the presence of one quinone moiety. However, all the compounds showed one violations in Lead likeness due to greater values for XLOGP3.

Table 3: Drug Likeness evaluation of hydrazones (Q-1 to Q-5)

Rule-based filters	**Q1**	**Q2**	**Q3**	**Q4**	**Q5**
Lipinski violations	0 violation	0 violation	0 violation	0 violation	0 violation
Ghose violations	0 violation	0 violation	0 violation	0 violation	0 violation
Veber violations	0 violation	0 violation	0 violation	0 violation	0 violation
Egan violations	0 violation	0 violation	0 violation	0 violation	0 violation
Muegge violations	0 violation	0 violation	0 violation	0 violation	0 violation
Bioavailability Score	0.55	0.55	0.55	0.55	0.55
PAINS No. of Alerts	1 alert: chinone_A	1 alert: chinone _A	1 alert: chinone_A	1 alert: chinone_A	1 alert: chinone_A
Brenk No. of Alerts	2 alerts: chinone_1, imine_1	2 alerts: chinone_1, imine_1	2 alerts: chinone_1, imine_1	2 alerts: chinone_1, imine_1	2 alerts: chinone_1, imine_1
Lead likeness No. of Violations	No; 1 violation: XLOGP3 >3.5	No; 1 violation: XLOGP3 >3.5	No; 1 violation: XLOGP3 >3.5	No; 1 violation: XLOGP3 >3.5	No; 1 violation: XLOGP3 >3.5
Synthetic accessibility	3.68	3.60	3.71	3.92	3.81

The Bioavailability Radar gives a first glance at the drug-likeness of the compounds. The pink area represents the optimal range for each property (lipophilicity: XLOGP3 between −0.7 and +5.0, size: MW between 150 and 500 g/mol, polarity: TPSA between 20 and 130 Å2, solubility: log S not higher than 6, saturation: fraction of carbons in the sp3 hybridization not less than 0.25, and flexibility: no more than 9 rotatable bonds. Thus, these preliminary results provide the lead for the design of more potent drug. Furthermore, the bioavailability radar of the compounds is given in **Figure 4**, and the colored zone depicts suitable physicochemical space for oral bioavailability.

Target Prediction:

The target prediction of all compounds was performed using the SwissTargetPrediction platform and the results are depicted as a pie-chart. The Q-1, containing phenyl ring linked to quinone through azomethine bond was predicted as 26.7% protease. All other derivatives Q-2 to Q-5, containing nitrogen, oxygen and sulphur atoms in ring were predicted as enzymes inhibitors with varying percentages, as given in **Figure 5**.

Molecular docking:

To predict interactions between proteins and small molecules is essential for advancing drug development, identifying various biological processes and comprehending protein functions. A powerful approach for this purpose is protein-ligand blind docking, which identifies protein binding regions, and foretelling a molecule's binding pose. The COX pathway has been linked to the development of different types of inflammations. The COX is expressed at very low levels under normal conditions, however, gets over-expressed during the inflammatory process, pathogenic stimuli and cancer progression. In order to understand the plausible binding affinities, we have conducted a molecular docking study of the synthesized analogs in the active site of human cyclooxygenase enzyme (COX-2) with PDB ID: 6COX downloaded from Royal Society Protein Data Bank (https://www.rcsb.org) using CB-Dock2 an online docking tool.

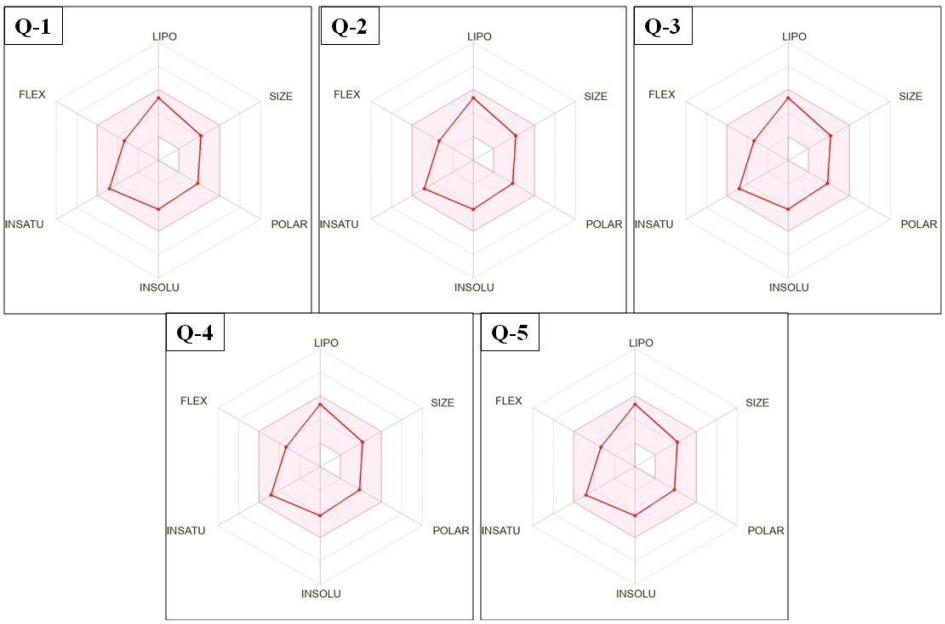

Figure 4: The Bioavailability Radar of hydrazones (Q-1 to Q-5)

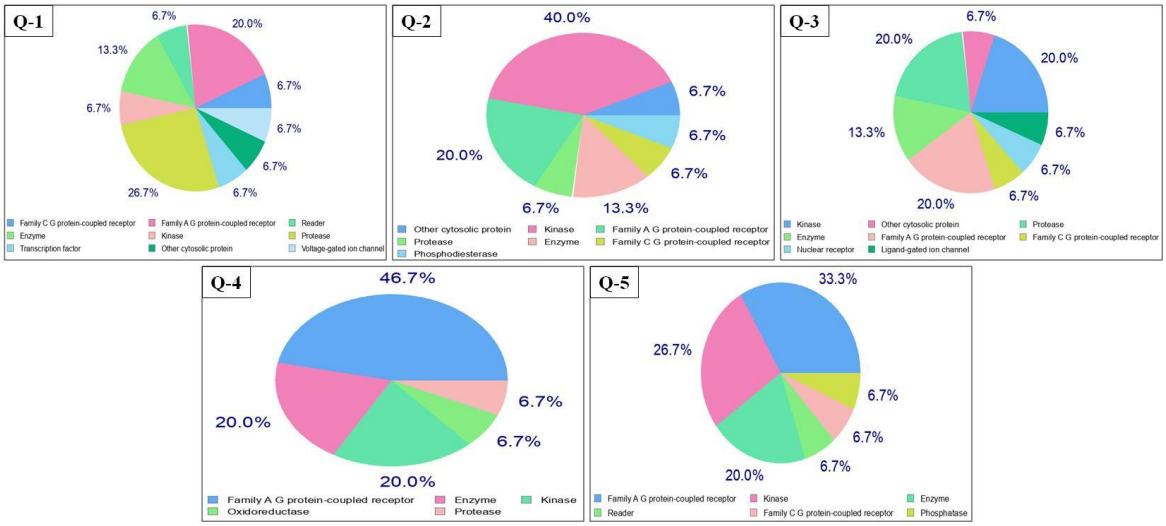

Figure 5: SwissTargetPrediction of hydrazones (Q-1 to Q-5)

We have conducted a molecular docking study of the synthesized analogs in the active site of human cyclooxygenase enzyme (COX-2) with PDB ID: 6COX downloaded from Royal Society Protein Data Bank (https://www.rcsb.org) using CB-Dock2 an online docking tool.The estimated binding energy values and the interacting amino acid residues are given in **Table 4**. The obtained values of binding energies reveal that all the synthesized hydrazones fit satisfactorily into the site of 6COX displaying hydrogen bonding with different amino acid residues of the target protein. The free binding energy for these derivatives was found to be in the range of -8.4 to -10.4 kcal/mol. The 3D and 2D diagrams of interactions with the amino acid side chains of the target protein is shown in **Figure 6**and **Figure 7.**

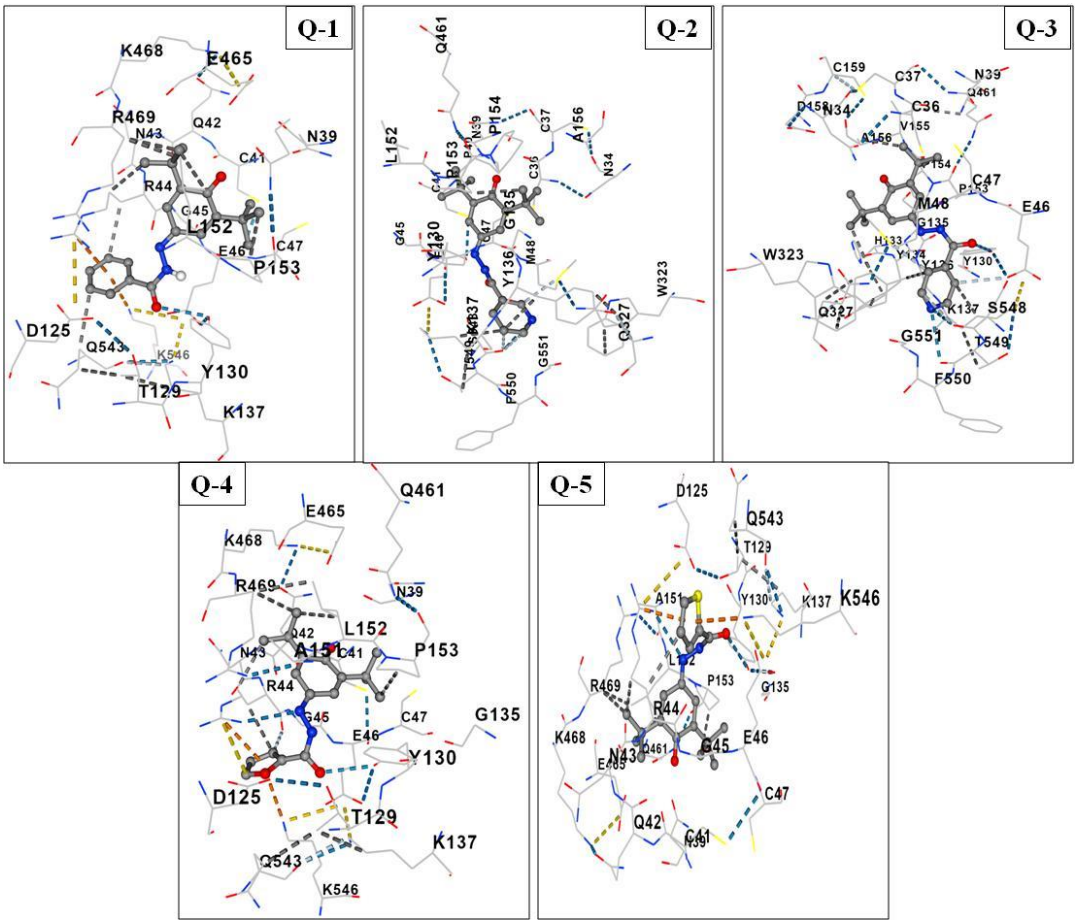

Figure 6: 3D-Binding modes of hydrazones (Q-1 to Q-5) in the active binding site of COX-2 Protein

The best docking score of -10.4 Kcal/mol was shown by derivatives Q-2 and other analogs showed a docking score between -8.4 to -9.3 Kcal/mol. All the designed compounds showed well established H-bonding with different amino acid residues. The binding free energy and other details from docking studies are presented in **Table 4**. Thus, the compound Q-2 has stronger binding interactions with 6COX than other derivatives.Most of the compounds established H-bond with different amino acid residues **(Figure 7)**.

The hydrazone, **Q-2** has the best binding energy since it established number of H-bonds throughout the whole extended molecule, and such binding mode should have made the molecule well-fixed in the protein active site. **Q-1** and **Q-3** also seem to have rigid poses, and each of them establishes various bonding interactions with different amino acid residues as shown in above table. From this, it can be concluded that the best among the five compounds employed in this study, the analog **Q-2** binds more strongly in the protein pockets and showed good interactions. Similarly, the remaining compounds also exhibited reasonably good interactions with the binding site amino acid residues with a good binding energy. Based on these results, compound **Q-2** has better stability in the COX-2 protein cavity than other analogs and hence, anticipated to show more enhanced antioxidant activity.

Table 4: Molecular docking results of hydrazones (Q-1 to Q-5)

No.	**Compound**	**Binding Energy (Kcal/Mol)**	**Binding amino acid residues**

1	Q-1	-9.3	ASN39, CYS41, GLN42, ASN43, ARG44, GLY45, GLU46, CYS47, ASP125, THR129, TYR130, LYS137, LEU152, PRO153, GLN461, GLU465, LYS468 and ARG469.
2	Q-2	-10.4	ASN34, CYS36, CYS37, ASN39, PRO40, CYS41, GLY45, GLU46, CYS47, MET48, TYR130, GLY135, TYR136, LYS137, LEU152, PRO153, PRO154, ALA156 and GLN461.
3	Q-3	-9.1	ASN34, CYS36, CYS37, ASN39, GLU46, CYS47, MET48, TYR130, HIS133, TYR134, GLY135, TYR136, LYS137, PRO153, PRO154, VAL155, ALA156, ASP158, CYS159 and GLN461.
4	Q-4	-8.8	ASN39, CYS41, GLN42, ASN43, ARG44, GLY45, GLU46, CYS47, ASP125, THR129, TYR130, GLY135, LYS137, ALA151, LEU152, PRO153, GLN461, GLU465, LYS468 and ARG469.
5	Q-5	-8.4	ASN39, CYS41, GLN42, ASN43, ARG44, GLY45, GLU46, CYS47, ASP125, THR129, TYR130, GLY135, LYS137, ALA151, LEU152, PRO153, GLN461, GLU465, LYS468 and ARG469.

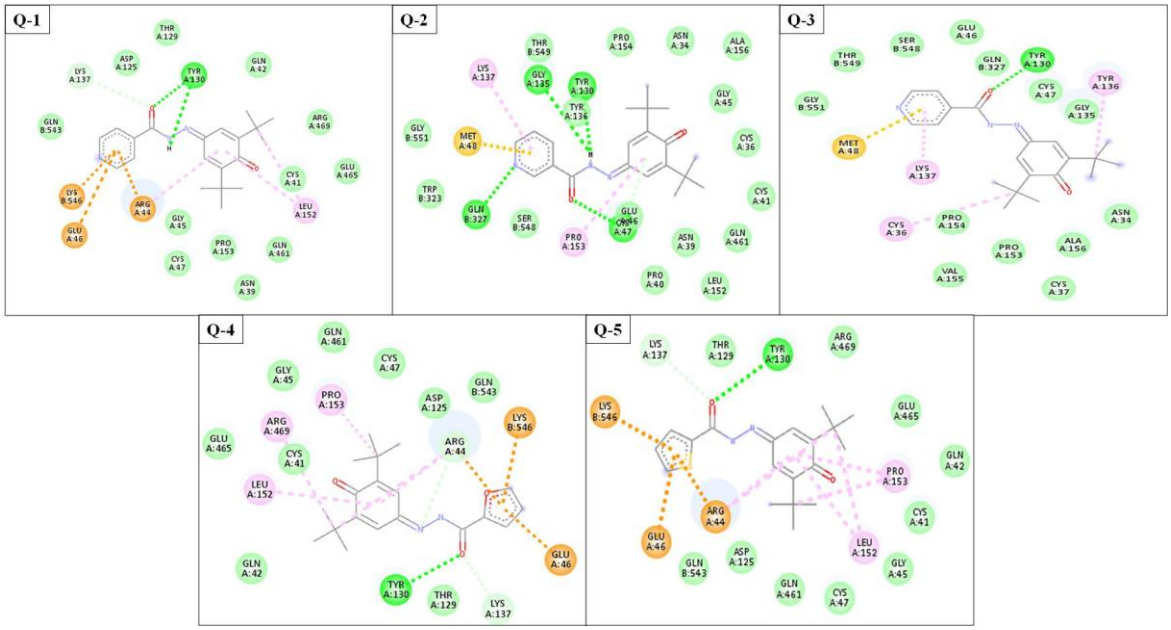

Figure 7: 2D-Interaction analysis of hydrazones (Q-1 to Q-5) in the active binding site of COX-2 Protein

CONCLUSION:

In the present study, we have successfully synthesized the biologically active hydrazones **Q-1 to Q-5** from 2,6-di-tert-butyl-1,4-benzoquinone and hetero aromatic hydrazides. The structures of molecules were characterized and elucidated by LCMS and ^{1}H-NMR spectroscopic techniques. During the biological evaluations in terms of antioxidant potential, the hydrazone **Q-2** shows noteworthy antioxidant potential determined using DPPH radical scavenging method. All the derivatives were virtually screened for their ADMET, physicochemical, drug likeness and toxicity studies. All the compounds showed good pharmacodynamics, no violations in drug-likeness and devoid of cytotoxicity. These compounds were further

subjected for possible target prediction and the compounds were found to target enzymes. All compounds exhibited reasonably good interactions with amino acid residues and showed a good binding energy during molecular docking. The evaluated binding energy values indicated that all compounds fit favorably into the 6COX active site displaying hydrogen bonding with different amino acid residues of the target protein. The experimental of antioxidant activity fit well with the predicted *in silico* results. Therefore, these new derivatives containing a quinone and heterocyclic hydrazides joined through azomethine group can become good drug candidate for designing new drug.

ACKNOWLEDGEMENTS:

We are thankful to the Department of Science and Technology, Govt. of India for providing financial assistance under DST-FIST (0 Level) to Abeda Inamdar Senior College, Pune vide letter number SR/FST/COLLEGE-277/2018 dated 20th December 2018 and CIF, SPPU, Pune for providing the characterization data. We are grateful to Dr. P. A. Inamdar, the President of MCE Society, Pune for providing the lab facilities.

REFERENCES

i. Shah S. K.; Goyal A.; A review for biological activity on hydrazide hydrazones: A promising moiety; Eur. J. Mol. clinical med.; 2020, **07**(03), 857-881.

ii. Pangal A.; Ahmed K.; Synthesis, biological evaluation and molecular docking studies of C-3 substituted coumarin analogs to explore their anti-proliferative potential; Curr. Trends Biotechnol. Pharm.; 2023, **17**(1), 649-659.

iii. Pangal A.; Ahmed K.; Synthesis and biological evaluation of coumarin-quinone hybrids as multifunctional bioactive agents; ADMET and DMPK; 2022, **11**(1), 81-96.

iv. Shaterzadeh-Yazdi H.; Noorbakhsh M. F.; Hayati F.; Samarghandian S. and Farkhondeh T.; Immunomodulatory and anti-inflammatory effects of thymoquinone; Cardiovasc HematolDisord Drug Targets; 2018, **18**(1), 52-60.

v. Wellington K. W.; Kolesnikova N. I.; Nyoka N. B. P. and McGaw L. J.; Investigation of the antimicrobial and anticancer activity of aminonaphthoquinones; Drug Dev Res.; 2019, **80**(1), 138-146.

vi. Wellington K.W.; Understanding cancer and anticancer activities of naphthoquinones-a review; RSC. Adv.; 2015, **5**, 20309-20338.

vii. Bhasin D.; Chettiar S. N.; Etter J. P.; Mok M. and Li P. K.; Anticancer activity and SAR studies of substituted 1,4-naphthoquinones; Bioorg. Med. Chem.; 2013, **21**(15), 4662-4669.

viii. Paengsri W. and Baramee A.; Synthesis and evaluation of anti-tuberculosis and anti-cancer activities of hydroxynaphthoquinone derivatives; Chiang. Mai. J. Sci.; 2013, **40**(1), 70-76.

ix. Huang L. J.; Chang F. C.; Lee K. H.; Wang J. P.; Teng C. M. and Kuo S. C.; Synthesis and antiplatelet, antiinfammatory, and antiallergic activities of substituted 3-chloro-5,8-dimethoxy-1,4-naphthoquinone and related compounds; Bioorg Med Chem.; 1998, **6**(12), 2261-2269.

x. Lien J. C.; Huang L. J.; Teng C. M.; Wang J. P. and Kuo S. C.; Synthesis of 2-alkoxy 1,4-naphthoquinone derivatives as antiplatelet, antiinfammatory, and antiallergic agents; Chem Pharm Bull (Tokyo).; 2002, **50**(5), 672-674.

xi. Huang S. T.; Kuo H. S.; Hsiao C. L. and Lin Y. L.; Efficient synthesis of "redoxswitched" naphthoquinone thiol-crown ethers and their biological activity evaluation; Bioorg Med Chem.; 2002, **10**(6), 1947-1952.

xii. Sasaki K.; Abe H. and Yoshizaki F.; In vitro antifungal activity of naphthoquinone derivatives; Biol Pharm Bull.; 20002, **25**(5), 669-670.

xiii. Jin Y. R.; Ryu C. K.; Moon C. K.; Cho M. R. and Yun Y. P.; Inhibitory effects of J78, a newly synthesized 1,4-naphthoquinone derivative, on experimental thrombosis and platelet aggregation; Pharmacology.; 2004, **70**(4), 195-200.

xiv. Inbaraj J. J. and Chignell C. F.;Cytotoxic action of juglone and plumbagin: a mechanistic study using HaCaT keratinocytes. Chem Res Toxicol.; 2004, **17**(1), 55-62.

xv. Yuk D. Y.; Ryu C. K.; Hong J. T.; Chung K. H.; Kang W. S. et al; Antithrombotic and antiplatelet activities of 2-chloro3-[4-(ethylcarboxy)-phenyl]-amino-1,4-naphthoquinone (NQ12), a newly synthesized 1,4-naphthoquinone derivative; BiochemPharmacol.; 2000, **60**(7), 1001-1008.

xvi. Sharma S. and Utreja D.; Synthesis and antiviral activity of diverse heterocyclic scaffolds; Chem. Biol. Drug Des.; 2021, **99**(01), 870-920.

xvii. Jain N.; Utreja D.; Kaur K. and Jain P.; Novel derivatives of nicotinic acid as promising anticancer agents; Mini Rev. Med. Chem.; 2021, **21**(7), 847-882.

xviii. EmamiS. and Dadashpour S.; Current developments of coumarin-based anti-cancer agents in medicinal chemistry; Eur. J. Med. Chem.; 2015, **102**, 611-630.

xix. Patil P.; Sethy S. P.; Sameena T. and Shailaja K.; Pyridine and Its Biological Activity, A Review; Asian J. Research Chem.; 2013, **6**(10), 888-899.

xx. Khalaf H. S.; Tolan H. E. M.;, El-Bayaa M. N.; Radwan M. A. A.; El-Manawaty M. and El-Sayed W. A.; Synthesis and anticancer activity of new pyridine-thiophene and pyridine-furan hybrid compounds, their sugar hydrazone, and glycosyl derivatives; Russ. J. Gen. Chem.; 2020, **90**, 1706-1715.

xxi. Dan L.; Ya Z.; Qin L.; Juan L.; Qihua J.; Baicheng H. and Qiang T.; Synthesis, in vitro antitumor activity and molecular mechanism of novel furan derivatives and their precursors"; Anti-Cancer Agents in Med. Chem.; 2020, **20**(12), 1475-1486.

xxii. Paul K.; Bindal S. and Luxami V.; Synthesis of new conjugated coumarin–benzimidazole hybrids and their anticancer activity; Bioorg. Med. Chem. Lett.; 2013, **23**, 3667-3672.

xxiii. Sashidhara K. V.; Kumar A.; Kumar M.; Sarkar J. and Sinha S; Synthesis and in vitro evaluation of novel coumarin–chalcone hybrids as potential anticancer agents; Bioorg. Med. Chem. Lett.; 2010, **20**, 7205-7211.

xxiv. Pangal A.; Shaikh J.; Gazge M.; Mane V. and Ahmed K;Novel 3-acetylcoumarin schiff's base synthesis from different acid hydrazide; Int. Res. J. Pharm.; 2013, **4**, 108-110.

xxv. Pangal A.; Tambe P. and Ahmed K.; Screening of 3-acetylcoumarin derivatives as multifunctional biological agents; Current chemistry letters; 2023, **12**, 343-352.

xxvi. Dulo B.; Phan K.; Githaiga J. et al; Natural Quinone Dyes: A Review on Structure, Extraction Techniques, Analysis and Application Potential; Waste Biomass Valor; 2021, **12**, 6339-6374.

xxvii. Shaikh J.; Pangal A. and Ahmed K.; Design and *in silico* evaluation of new azo barbituric acid analogs as possible anticancer agents; Hetercyclic letters; 2022, **12**(4), 725-735.

Received on August 15, 2023.